Vol. 42, No. 3 (2020) 468-480, DOI: 10.24874/ti.866.04.20.07

Tribology in Industry

www.tribology.rs

RESEARCH

Effect of Ni-Coated Reinforcement on Mechanical and Tribological Properties of Heat Treated Aluminium Composite

S. Prabhu[a], P.H. Durga Prasad[a], N. Radhika[a,*]

[a] *Department of Mechanical Engineering, Amrita School Engineering, Coimbatore, Amrita Vishwa Vidyapeetham, India.*

Keywords:

Liquid metallurgy
Electroless nickel coating
Heat treatment
Dry sliding wear
Taguchi method

* Corresponding author:

N. Radhika
E-mail: n_radhika1@cb.amrita.edu

Received: 1 April 2020
Revised: 26 May 2020
Accepted: 27 July 2020

A B S T R A C T

The present work focusses on improving the mechanical and tribological properties of Al-5Si-3Cu alloy and Ni-coated TiC reinforced composite fabricated through liquid metallurgy route, through T6 heat treatment. Good interfacial bonding was developed between the matrix and coated reinforcement on microstructural investigation. There was an improvement in hardness for heat-treated alloy and composite by 34.5% and 14.7% respectively. Tensile strength for heat-treated alloy and composite was enhanced by 25.9% and 30.6% respectively. Pin on disc dry sliding wear test was carried out for Ni-coated TiC heat-treated composite for varying loads (10, 20, 30N), distances (500, 1000, 1500m) and velocities (1, 2, 3m/s) by using Taguchi's L27 Orthogonal Array. It was concluded that load had the highest influence on wear rate (71.88%), whereas the effects of sliding distance (8.23%) and velocity (3.45%) were nominal. Wear analysis revealed that, wear rate increased with an increase in load and sliding velocity and decreased with increasing sliding distance. Defects like delamination, grooving, and protrusions were observed on the worn surface. Thus, this kind of Ni-coated TiC reinforced composites can be used in camshafts, bearings and bushes for better wear resistance.

1. INTRODUCTION

Al-Si-Cu alloys are well known for their extensive properties like machinability and cast-ability due to the presence of aluminium (Al) and silicon (Si), moderate wetting properties, good tensile strength and corrosion resistance provided by the presence of copper (Cu). These alloys are widely used in automotive industrial applications such as gearboxes, cylinder heads, crankcases, tool handles and compressor housings [1]. Vandersluis et al. experimental results showed that the pre-heating temperature of mold had a significant effect on the solidification rate, secondary dendrite arm spacing (SDAS) and hardness. It was concluded that pre-heating temperature was directly proportional to SDAS and inversely proportional to hardness and solidification rate [2]. Researchers have concluded that Al-Si-Cu alloys

have columnar dendritic structure of α-silicon (α-Si) [3,4]. Jayakumar et al. concluded that α-Si underwent grain modification to fine grain structure on moving towards the outer periphery of cast specimen fabricated through centrifugal casting process [5].

Al alloys are known for their enhanced properties on addition of reinforcement particles like Boron Carbide (B_4C), Aluminum Oxide (Al_2O_3), Silicon Carbide (SiC), Titanium Carbide (TiC), Zirconia (ZrO_2), graphene and fly ash particles [6,7]. Kennedy et al. found that on addition of large volume percentage of TiC and Titanium Boride (TiB_2) particles led to the refinement of grain structure at some localities, which affected the mechanical properties [8]. Microstructural analysis of Al/TiC composite obtained by reactive synthesis route revealed the absence of clusters and confirmed the uniform distribution of reinforcements in the composite matrix [9]. It was reviewed that bonding and phases formed between matrix and reinforcement played a crucial role in enhancing the properties of composites [10-12]. Coatings on reinforcements increased the potentiality of composites and it helped in boosting the mechanical properties [13]. Lei Fan et al. investigation revealed that the quality of nickel (Ni) coating on ZrO_2 toughened the Al_2O_3 (ZTA) particles when temperature was varied and at 85 °C, a uniform coating was observed on ZTA particles [14]. Zou's research concluded that the Ni-coated SiC reinforcements in aluminium composite reduced the porosity, improved the corrosion resistance and enhanced self-passivation ability to a greater extent [15]. Experimental studies also concluded that copper (Cu) coated reinforcement particles addition boosted the tensile and hardness properties of Al alloy [16,17]. It was observed that the homogeneity of anodized coating was affected by the size of reinforcement particle [18]. In wear analysis of Al/SiC-C hybrid composite, it was inferred that Ni-coated reinforced composite exhibited better results than Cu and also precipitate formation was observed when coated particles were added. These precipitates enhanced the hardness and minimized the wear rate [19]. Researchers concluded that dry sliding wear rate increased with load in Al composites [20,21].

Based on the literature studies, it was observed that, wear analysis of Al-5Si-3Cu alloy using L27 Taguchi's optimization technique was limited. Hence, the present study deals with the fabrication of Al-5Si-3Cu/Ni-coated TiC composite and subjecting it to T6 heat treatment process. Metallography, mechanical and tribological analysis were performed. A comparative analysis was done for non-heat treated (NHT) and heat-treated (HT) alloy and composite.

2. MATERIALS AND METHODS

This section clearly explains the process involved in material selection and the experimental steps involved in the fabrication of the alloy and composite. The main objective is to enhance the bonding between Al-Si-Cu alloy and reinforcement particles. Al-5Si-3Cu alloy was preferred, considering Cu wettability and its wide range of applications in light structures and mild wear areas. Keeping view on the need for properties like high wear and temperature resistance, Titanium Carbide (TiC) of standard size of 44 μm (325 mesh) and average purity of 91 % was chosen as the reinforcement material. The reinforcement particles are bought from a Coimbatore Metal Mart Pvt. Ltd., India.

2.1 Electroless Nickel coating on TiC particles

Initially, TiC particles were thoroughly cleaned with acetone to remove any dust presence and prevent the particles from undergoing oxidation. The particles were then roughened using aqueous solution HNO_3 (100 ml/l) to easily coat the reinforcement particles. Sensitization was done in the presence of an aqueous solution of $SnCl_2$ (10 g/l) and HCl (25 ml/l) and activation was done in a solution of $PdCl_2$ (0.30 ml/l) and HCl (3 ml/l). The bath solution consisted of $NiCl_2$ (50 g/l), sodium hypophosphite (7 g/l), trisodium citrate (80 g/l) and ammonium chloride (50 g/l). The pH of the bath was found to be 9. The activated TiC particles were then dipped in a bath at a temperature of 75-80 °C for 45 min and dried in an oven at 60 °C for 1 hour. Scanning Electron Microscopy (SEM) and Energy Dispersive X-ray spectroscopy (EDX) were performed on Ni-coated TiC (Ni-TiC) reinforcement particles.

2.2 Fabrication of alloy and composite

As the first step, the graphite crucible was cleaned and pre-heated (350 °C, 30 minutes) to

remove any moisture and oily substances present in the crucible. Al-5Si-3Cu alloy was placed in a crucible and positioned in an electric furnace. The alloy was then allowed to melt at a temperature of 770 °C in the presence of argon (Ar) gas to avoid formation of any unwanted chemical compounds. The metallic die was pre-heated to 250 °C, to eradicate metal shrinkage while pouring the molten metal. Once the alloy had melted, molten metal was poured into the pre-heated metallic die and allowed to solidify at room temperature. After solidification, the cast product of Al-5Si-3Cu alloy in the cylindrical shape of Ø20 mm x 150 mm was obtained. To fabricate composite, pre-heated (200 °C) Ni-TiC of 6 wt.% reinforcement was added and stirred at a speed of 250 rpm for uniform distribution of TiC particles. The remaining process was carried out as mentioned above and Al-5Si-3Cu/Ni-TiC composite was obtained. The elemental composition of Al-5Si-3Cu alloy is shown in Table 1.

Table 1. Elemental composition of Al-5Si-3Cu alloy.

Element	Al	Si	Cu	Fe	Mn	Zn	Ni
As-cast Al-5Si-3Cu (wt.%)	Bal	5.3	3.1	0.6	0.3	0.34	0.02

2.3 Heat-treatment

Standard T6 heat treatment parameters provided by the ASTM for Al-Si alloys were preferred as the specific process conditions. The process includes solutionizing followed by artificial aging for both alloy and composite specimens. The specimens were solutionized at 540 °C for 10 hours and quenched in water at room temperature. The quenched samples were age hardened at 165 °C for 10 hours and then air quenched at room temperature.

2.4 Experimental procedures

All the specimens were initially ground and polished with 1000 grit size emery paper. Velvet cloth polishing was performed using fine alumina powder and the specimens were later etched with Keller's reagent. The metallographic analysis was performed on Zeiss Axiovert 25 CA Inverted Metallurgical Microscope as per the ASTM E3-11 standard. Hardness test was performed on Vickers Hardness Tester Mitutoyo 201-101E at a load of 100 gf for a dwell time of 15 seconds as per the ASTM E384-11 standard. Tensile specimens were prepared as per the ASTM B 557M standard with a gauge length of 36 mm and the test was performed on Tinius Olsen H25KT Universal Testing Machine. After the tensile test, fractography analysis was conducted. Taguchi's Design of Experiments (DOE) was used to analyze the wear behavior of HT Ni-coated reinforced composite, as this had enhanced mechanical properties. Wear study was performed using a pin on disc tribometer of EN32 stainless steel counter disc (HRC70), based on the mass loss method without lubrication at room temperature according to the ASTM99-04 standard. The specimens of 12 mm diameter and 25 mm length were prepared for the wear test. Acetone was used to clean the specimen before and after each test, and mass loss was calculated. SEM analysis was also performed to analyze the worn surface.

3. RESULTS AND DISCUSSION

The metallographic analysis, mechanical properties such as hardness and tensile strength, wear behaviour, the statistical analysis and worn surface morphology are clearly explained in the following subsections.

3.1 SEM and EDX analysis of Ni-TiC

SEM analysis (Fig. 1a) was performed on Ni-coated TiC particles, which confirmed a uniform coating of Ni over TiC particles. The average size of the reinforcement particle after coating was observed as 56 μm. EDX analysis (Fig. 1b) confirmed the presence of Ni along with Ti and C. Based on this, it was concluded that a successful coating of Ni was made over TiC reinforcement particles through electro less coating process.

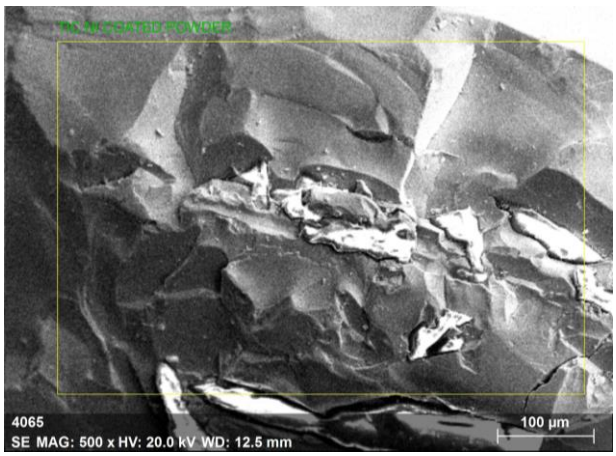

(a)

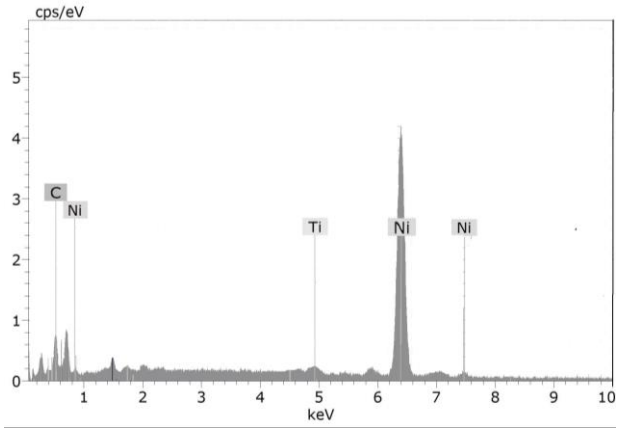

(b)

Fig. 1 (a) SEM of Ni-TiC particle (b) EDX of Ni-TiC particle.

3.2 Metallographic analysis

Figures 2a-2d show the microstructures (100x magnification) of both NHT and HT Al-5Si-3Cu alloy and Al-5Si-3Cu/Ni-TiC composite. From Fig. 2a, it was concluded that acicular grains of α-Si were clearly observed in the NHT Al-5Si-3Cu alloy, which deviated the properties of a material. α-Si was clearly surrounded by the α-Al phase. NHT Al-5Si-3Cu/Ni-TiC composite microstructure (Fig. 2b) clearly showed the presence of Ni-TiC particles, which were clearly distributed over the matrix phase. It was observed that composites underwent slight modification in microstructure owing to the grain refinement property of Ti-based reinforcement particles, similar behavior was observed in previous studies [18]. TiC particles refined α-Si to a certain extent. α-Si underwent modification to spherodized eutectic Si form in both HT samples (Figs. 2c-2d). During heat treatment, dislocation formation took place due to the thermal difference between α-Al and α-Si. This dislocation provided a vacant space for spherodized α-Si phase to occupy during solution treatment and aging [22].

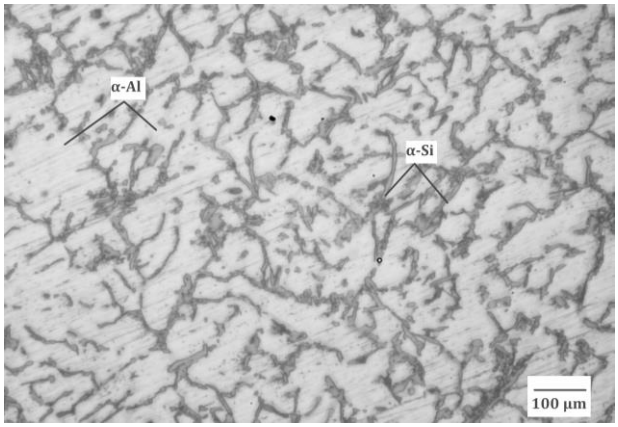

(a)

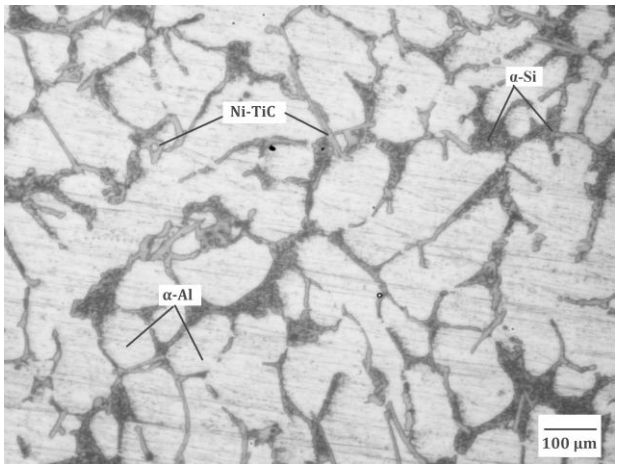

(b)

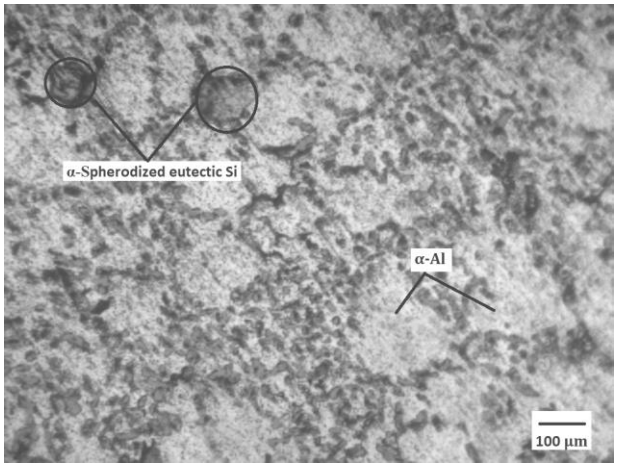

(c)

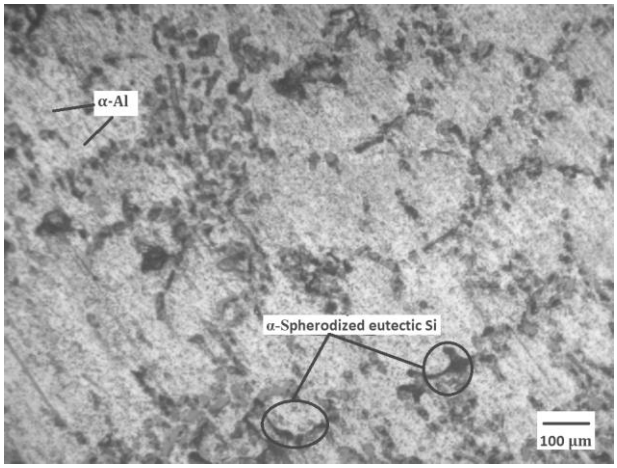

(d)

Fig. 2 Microstrucure of (a) NHT Al-5Si-3Cu alloy, (b) NHT Al-5Si-3Cu/Ni-TiC, (c) HT Al-5Si-3Cu alloy, and (d) HT Al-5Si-3Cu/Ni-TiC composite.

Formation of spherodized eutectic Si indicated that heat treatment of the T6 cycle was effective on both Al-5Si-3Cu alloy and Al-5Si-3Cu/Ni-TiC composite. This helped in boosting the properties of alloy and composite. Fine distribution of Ni-TiC was also observed in HT composite. X-ray diffraction analysis of NHT Al-5Si-3Cu/Ni-TiC

composite (Fig. 3) confirmed the presence of TiC particles, Al_2Cu phase and elements like Al and Si, whereas in HT Al-5Si-3Cu/Ni-TiC composite (Fig. 4), formation of meager Mg_2Si phase was confirmed alongside Al_2Cu phase, TiC, Al and Si.

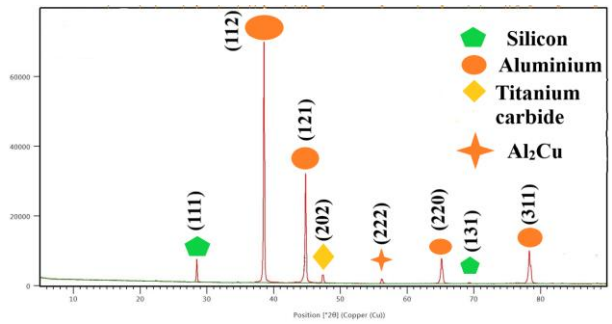

Fig. 3 XRD analysis of NHT Al-5Si-3Cu/Ni-TiC composite.

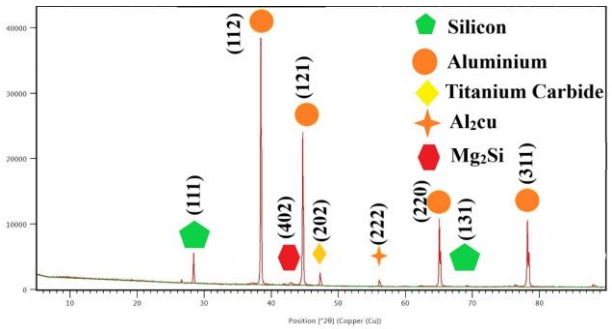

Fig. 4 XRD analysis of HT Al-5Si-3Cu/Ni-TiC composite.

3.3 Hardness analysis

Figure 5 clearly depicts the hardness values of all the samples (alloy and composite). Hardness was taken as an average of five different test locations. HT alloy exhibited a hardness of 128.2 HV, which was 28.2 % higher than NHT alloy.

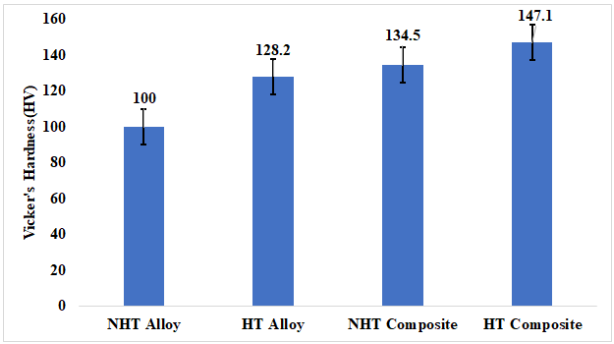

Fig. 5. Hardness of alloy and composite.

Similarly, HT composite had improved hardness of 147.1 HV which was 9.36 % better than NHT composite. Composites exhibited better hardness than their respective alloys as the load applied gets distributed homogenously over both matrix phase and reinforcement phase, which enhanced the ability of composites to absorb more load [23, 24]. Ti-based reinforcement particles have the ability of grain refinement, which also contributed to the enhancement of hardness values [19]. TiC coated with Ni improved the interfacial bonding properties, which resulted in enhanced hardness values [25]. Similar kinds of observations were made in the work of Huang [26] and Balaraju [27]. Both HT alloy and composite exhibited better hardness values due to breakage of α-Si acicular grains to undergo spherodization, and formation of Mg_2Si in HT samples helped in boosting hardness values [27].

3.4 Tensile strength analysis

The average tensile strength values of both NHT and HT samples are shown in Fig. 6. The tensile strength of HT Al-5Si-3Cu alloy increased by 25.9 % when compared to NHT Al-5Si-3Cu alloy.

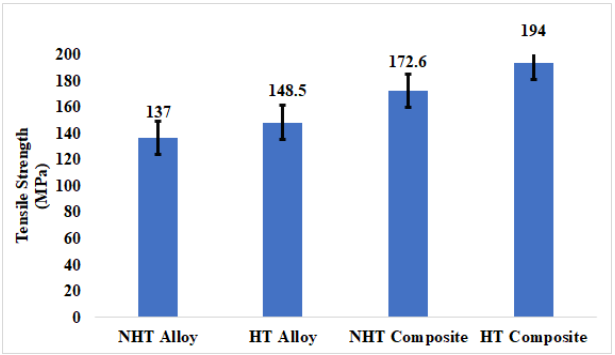

Fig. 6 Tensile strength of alloy and composite.

The tensile strength of HT Al-5Si-3Cu/Ni-TiC composite was enhanced by 30.6 % when compared to NHT composite. Both the HT samples exhibited better strength due to spherodization of α-Si and this spherodized eutectic Si tended to act as an obstacle for the propagation of crack [28]. The major contribution of enhanced strength in composites was due to the wetting provided by Ni coating to TiC. During HT, due to differences in coefficient of expansion between alloy and reinforcement, dislocation density of Si increased, which promoted the strength and ductility of HT Al-5Si-3Cu/Ni-TiC composite [22].

3.5 Fractography analysis

To identify the type of fracture, fractography analysis was performed on HT Al-5Si-3Cu alloy and Al-5Si-3Cu/Ni-TiC composite using SEM. HT

Al-5Si-3Cu alloy (Fig. 7a) clearly showed the formation of facets and small cleavages which indicated brittle mode of failure with no evidence of ductile nature.

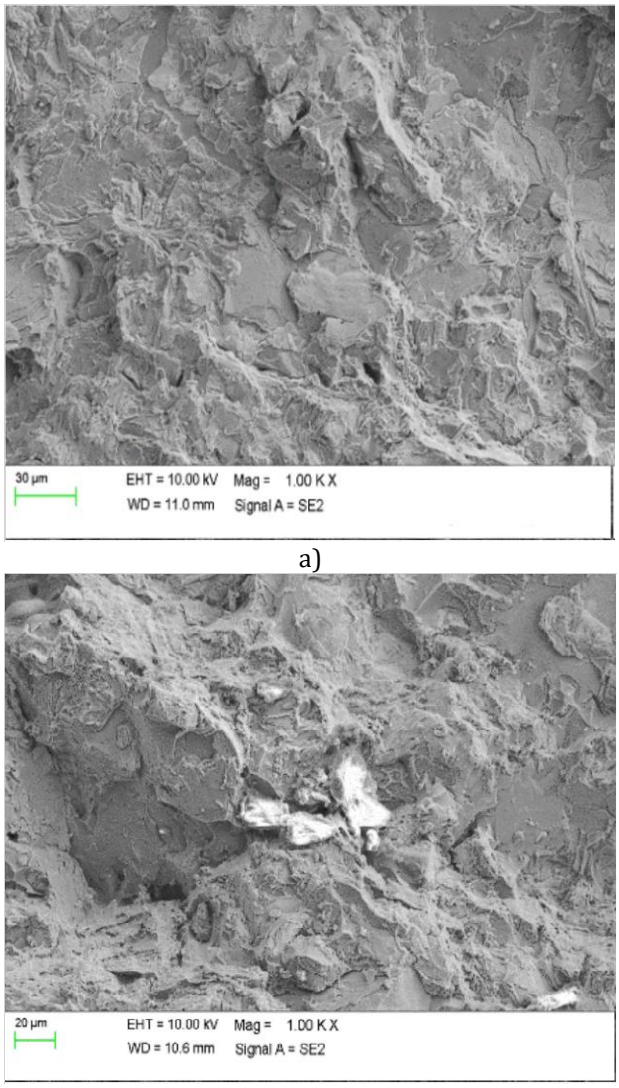

Fig. 7. a) Fractography analysis of HT Al-5Si-3Cu alloy, and b) Fractography analysis of HT Al-5Si-3Cu composite.

HT Al-5Si-3Cu/Ni-TiC (Fig. 7b) revealed the formation of dimples associated with minor flakes with no evidence of necking. These dimples and faces acted as crack initiators and stress concentrators, which caused brittle failure. Dimples were formed due to the detachment of reinforcement particles from the matrix phase [28].

4. DRY SLIDING WEAR ANALYSIS

HT Al-5Si-3Cu/Ni-TiC composite was only considered for wear analysis as it exhibited better mechanical properties than all other samples under study.

4.1 Taguchi Design of Experiments

Dry sliding wear analysis of HT Al-5Si-3Cu/Ni-TiC composite was conducted using Taguchi's DOE. Taguchi's DOE helps to get most accurate information with a minimum number of experiments. Using an Orthogonal Array (OA) for forming a matrix, it aids in studying the influence of multiple controllable factors on the average of quality characteristics and variations. L27 OA is used to analyse the results of the wear tests performed and the corresponding wear rates obtained are shown in Table 2.

Table 2. Results of L27 Orthogonal Array.

Load (N)	Distance (m)	Velocity (m/s)	Wear rate (mm^3/Nm)
10	500	1	0.00030
10	500	2	0.00017
10	500	3	0.00015
10	1000	1	0.00015
10	1000	2	0.00026
10	1000	3	0.00011
10	1500	1	0.00027
10	1500	2	0.00025
10	1500	3	0.00037
20	500	1	0.00087
20	500	2	0.00074
20	500	3	0.00090
20	1000	1	0.00044
20	1000	2	0.00076
20	1000	3	0.00083
20	1500	1	0.00047
20	1500	2	0.00067
20	1500	3	0.00074
30	500	1	0.00156
30	500	2	0.00172
30	500	3	0.00207
30	1000	1	0.00100
30	1000	2	0.00119
30	1000	3	0.00159
30	1500	1	0.00067
30	1500	2	0.00079
30	1500	3	0.00106

4.2 Signal-to-Noise (S/N) ratio analysis

To know the ranking order of the influencing parameters (distance, speed, load), S/N ratio analysis was performed (Table 3). The most influencing parameter is ranked based on the delta value. Delta value is obtained as the difference of highest and lowest S/N ratio. The largest delta valued parameter is the most effecting parameter on dry sliding wear. From

the results obtained, load was considered as the most prompting parameter followed by distance and velocity. Optimum values were determined from the S/N ratio plot (Fig. 8). The minimum wear rate was observed at 10 N load, 1000 m sliding distance and 1 m/s velocity.

Table 3. Response table for Signal-to-Noise ratio.

Level	Load (N)	Distance (m)	Velocity(m/s)
1	73.53	63.57	65.88
2	63.17	65.89	64.83
3	58.29	65.54	64.29
Delta	15.24	2.32	1.59
Rank	1	2	3

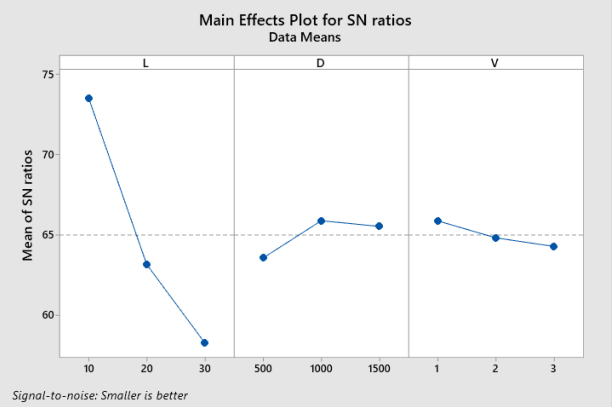

Fig. 8. Main effect plot for S/N ratio – Wear rate.

4.3 Effect of load on the wear rate

From Fig. 9, it was observed that the wear rate increased from 10 N to 30 N. At 10-20 N applied load, minimum wear rate was observed as the wear experienced by the sample due to the load was resisted by the Ni-coated TiC reinforced matrix.

Fig. 9. Main Effect plot for Mean – Wear rate.

This was mainly due to the strong interfacial bond strength developed between the Ni-coated TiC particle and the matrix, which aided in load transfer to the matrix. Also, the heat treatment of the material led to proper grain refined structure (fine) which boosted the ability of matrix to withstand load. As load increased, the contact area between disc and specimen increased as well. This tends to increase the temperature at the interface of the sample and disc. High temperature made the material soft at the contact area, thereby making it unable to withstand higher loads, which caused higher wear rates and surface damage. This factor contributed in increasing the wear on the surface. Due to higher loads, the reinforcement particles were squeezed out of the matrix. These particles get stuck between the surface of the disc and specimen, causing more wear on the surface. Similar observations were made by an author regarding load for Al composites [29-32].

4.4 Effect of distance on wear rate

As distance increased from 500 m to 1500 m, the wear rate decreased as well. At low sliding distance values i.e. 500 m, maximum wear rate was observed due to high temperature generated at the interface, which led to plastic deformation of the pin material. At 1500 m, minimal wear rate was observed, which was mainly due to the formation of Mechanical Mixed Layer (MML) [24]. Due to the higher distance and longer sliding duration, transfer of material took place from disc to sample. Material which underwent plastic deformation initially was peeled off as wear debris. The peeled off material underwent oxidization along with the new layer that comes in contact with the atmosphere. MML mainly consisted of oxides, which enhanced the potential of the specimen to withstand longer sliding distances and exhibit low wear.

4.5 Effect of velocity on wear rate

Wear rate increases with increase in velocity from 1 m/s to 3 m/s. At a velocity of 1 m/s, minimal damage to surface occurred due to the improved interfacial bonding with Ni-coated TiC particle and matrix. The reinforcement particles and the matrix were closely held together due to enhanced wettability characteristics provided by the Ni-coated TiC particles and the fine grain structure formed due to the T6 heat treatment.

Table 4. Selected parameters and their confirmation results.

S. No	Load (N)	Sliding distance(m)	Sliding velocity(m/s)	Regression wear rate(mm^3/Nm)	Experimental wear rate (mm^3/Nm)	Error (%)
1	13	525	1.5	4.90E-04	4.70E-04	4.08
2	19	900	1.6	7.51E-04	7.26E-04	3.32
3	24	1100	2.3	1.41E-04	1.01E-04	2.83

Table 5. Analysis of Variance.

Source	DF	Adj SS	Adj MS	F-Value	P-Value	P (%)
L	2	5.158E-06	0.000003	581.62	0.0000001	71.95
D	2	5.91E-07	0.000001	69.16	0.0000089	8.33
V	2	2.48E-07	0.000001	20.09	0.0007607	3.60
L*D	4	8.51E-07	0.000001	43.69	0.0000177	11.98
L*V	4	2.25E-07	0.000001	10.92	0.0025129	3.46
D*V	4	4.6E-08	0.000001	1.8	0.2229959	0.68
Error	8	5.6E-08	0.000001			0.78
Total	26	7.175E-06				100

Note: DF-Degree of Freedom, Adj ss-Adjacent Sum of Square, Adj MS-Adjacent Mean Square, F-Fisher Test, P- Probability, P (%)-Percentage contribution.

The combination of superior wettability, bonding strength and fine grain structure provided superior resistance to wear under action of deformation. Between 1 m/s and 3m/s, the wear slowly started increasing due to increase in temperature at the point of contact. The interfacial bonding strength which held the particles and matrix together began to weaken, which led to breakage of bonds and increase the rate of material removal. At high velocity i.e. 3 m/s, maximum wear was observed. Matrix softening occurred at higher velocities due to a rise in temperature, which led to plastic deformation of the material. This deformation makes the surface tend to lose the outer layer and worn out easily. The interfacial bonding strength developed between the reinforcement particle and the matrix began to fade and this leads to pullout of material from the matrix and exposed the fresh layers. Radhika et al. found similar trend in wear with respect to velocity [30,33,34]. As velocity increased, coefficient of friction also increased. This friction peeled off the outer layer and this increased the wear rate to a higher value.

4.6 Linear regression analysis and confirmation of experiment

The relationship among variables like sliding distance, load, and sliding velocity was estimated through regression analysis. These parameters were correlated and were used for calculating the wear rate, which was compared with the experimental wear value. The regression equation is as shown below.

$$WR = -0.000582 + 0.000079\ L - 0.000001\ D + 0.000211\ V - 0.000000\ L*D + 0.000013\ L*V + 0.000000\ D*V$$

where each variable denotes the following, D – sliding distance (m), L – applied load (N), and V – sliding velocity (m/s).

The increase in wear rate was represented by a positive sign and the decrease in wear rate by a negative sign. A comparison of experimental wear with regression wear rate was performed and the error percentages were listed in Table 4. From Table 4, it was inferred that error value was less than 5 %. Hence, it was confirmed that the experimental model has limited variance in predicting the wear behaviour.

4.7 Analysis of variance

To know the effect of each process parameter, Analysis of Variance (ANOVA) was performed in both qualitative and quantitative variables. The analysis was performed with a confidence level of 95 % and with a significance level of 5 %. The parameter with less than 0.05 P-value had more effect on the wear rate. From Table 5, it was confirmed that load (71.88 %) was the contributing factor on wear rate, followed by distance and velocity with 8.23 % and 3.45 % respectively.

5. WORN SURFACE ANALYSIS

The worn surface mechanism of HT Al-5Si-3Cu/Ni-TiC composite was interpreted through SEM analysis. At low load condition of 10 N (Fig. 10a), sliding velocity of 1 m/s and a sliding distance of 500 m, few locations displayed the presence of shallow grooves and scratches. Shallow grooves were formed parallel to surface of the track, as low load was insufficient to shear out material.

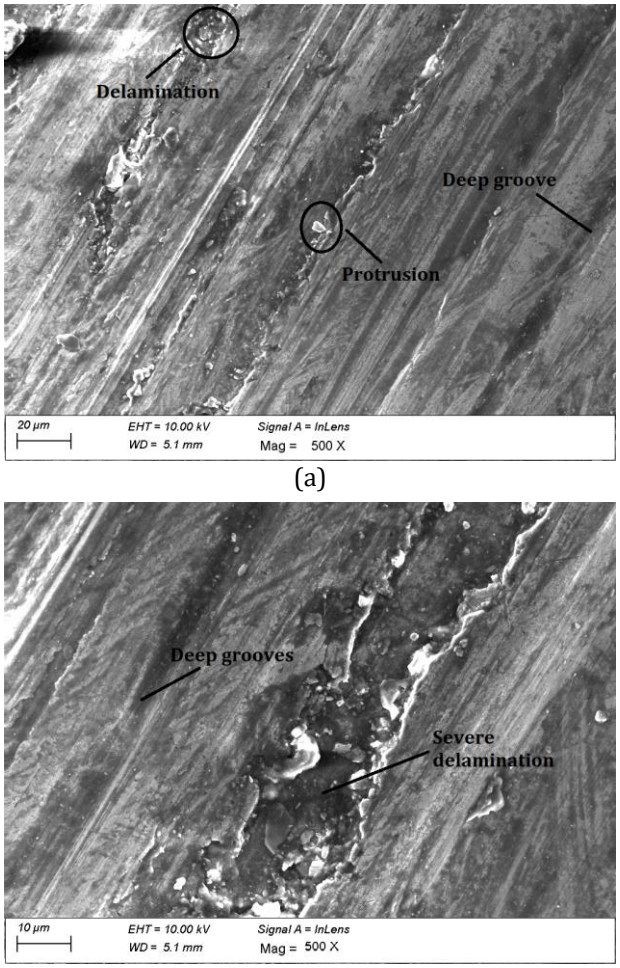

Fig. 10. SEM analysis of worn surface at different loads (a) 10 N, and (b) 30 N.

This minimal surface wear was mainly due to the superior resistance to deformation developed by the good interfacial bonding strength between the Ni-coated particle and matrix. Furthermore, the surface was devoid of any casting defects formed which was removed by the fine grain structure formed during heat treatment. Delamination mode of wear was observed at high load conditions (30 N, 500 m, 1 m/s) (Fig. 10b). Due to the ploughing mechanism, laminar layers were peeled out from subsurface causing deep grooves, when compared to low load conditions. Comparative analysis of Figs. 10a and 10b, it was concluded that the worn surface displayed very good wear resistance even at high load applications.

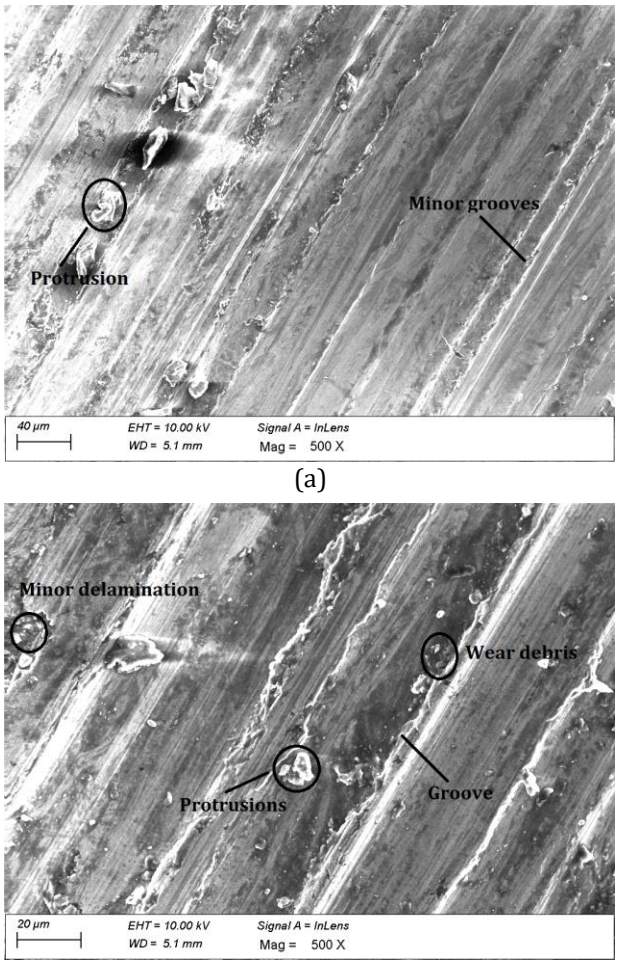

Fig. 11. SEM analysis of worn surface at different velocities (a) 1m/s, and (b) 3 m/s.

From Fig. 11a, a clear formation of minor grooves and protrusions were observed along the sliding direction at 1m/s sliding velocity, 1500 m distance and 10 N load. As the velocity was low, minimal damage to the surface occurred, due to the superior resistance to deformation produced by the high interfacial bonding strength between Ni-coated TiC reinforcement particles and fine grain matrix structure. As velocity increased to 3 m/s (Fig. 11b) the temperature at the contact vicinity also increased, which worsened the surface damage with features like delamination, and wear debris getting micro-welded to surface and grooves. On further action, these particles and micro-welds

get detached from the surface due to the weakening in the interfacial bonding strength between the particle and the matrix material. Any resistance offered by the matrix also decreased, which increased the rate of material removal and worsened the surface damage.

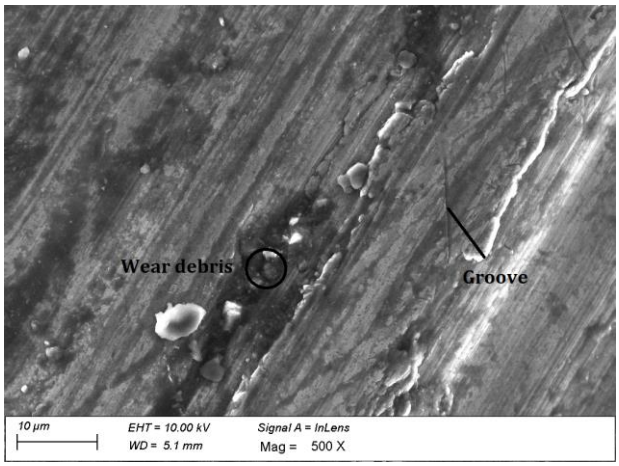

(a)

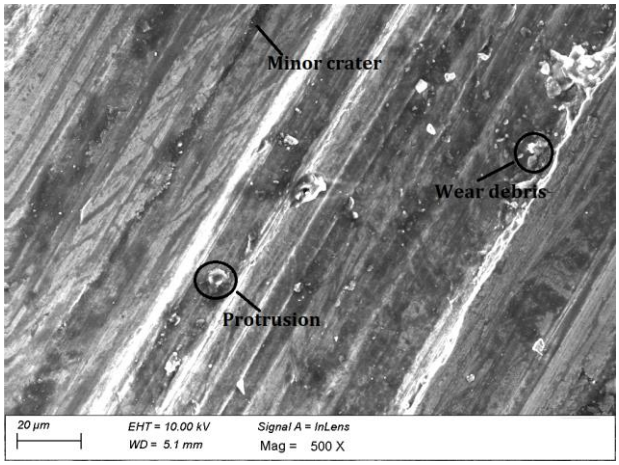

(b)

Fig. 12. SEM analysis of worn surface at different distances (a) 500 m, and (b) 1500 m.

Sliding distance was the least influencing parameter. Figure 12a shows the worn surface at low sliding distance (500 m) at constant 20N load and 1m/s velocity. Analysis revealed the formation of grooves, and wear debris stuck on the surface. Once the peripheral layer was scrapped off, the adhesive particle-matrix bond strength weakened and protruded the Ni-TiC reinforcement particles. These particles were then pulled off from the specimen surface layer due to the repetitive loads. This deepened the shallow grooves to fine grooves revealing a fresh layer of particles, which undergo uniform wear due to stress concentration after heat treatment [35,36]. As the sliding distance increased (1500 m), the wear rate decreased due to the slipping effect produced by the adhesion of specimen surface and undergo plastic deformation, as shown in Fig. 12b.

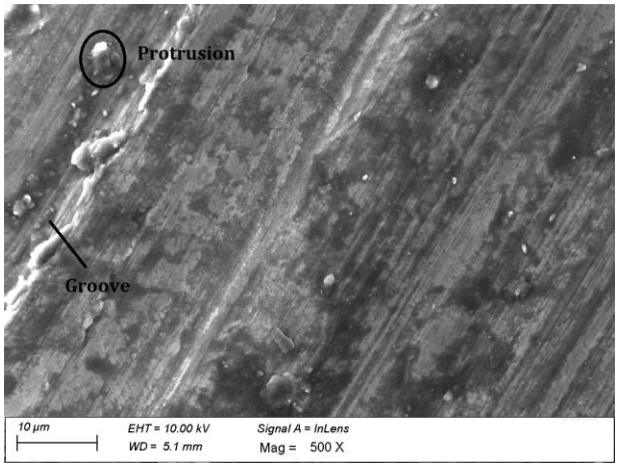

Fig. 13. SEM analysis of worn surface at L=10 N, V=1 m/s, D=1000 m.

Worn surface analysis of HT Al-5Si-3Cu/Ni-TiC composite (Fig. 13) at optimum process conditions (L=10 N, D=1000 m and V=1 m/s) was also performed. From SEM analysis, it was concluded that Ni-TiC particles were retained in the matrix at optimum condition. Grain boundary strength was enhanced due to HT, which resisted the wear rate. Shallow grooves alone were observed for the sample at optimum condition.

6. CONCLUSIONS

Al-5Si-3Cu alloy and Nickel coated TiC reinforced composite were fabricated through stir casting process. Microstructural, mechanical and wear analysis were performed on fabricated samples before and after heat treatment. Following conclusions were made.

- Ni-coated TiC particles had good interface bonding with aluminium matrix due to the improved wettability by Ni coating and thus enhancing the material properties.
- The hardness and tensile strength value of HT alloy increased by 28.2 % and 8.36 % respectively, compared to NHT alloy due to spheroidization of eutectic Si particles.
- The hardness and tensile strength value of heat treated composite increased by 9.36 % and 12.4 % respectively, compared to NHT composite due to the combined effect of

spheroidised eutectic Si particles produced due to heat-treatment and the presence of Ni-coated TiC particles.

- L27 Taguchi analysis concluded an increasing wear rate trend for applied load and sliding velocity, whereas a decreasing trend was observed with increasing sliding distance. Optimum wear process parameters (L=10 N, V=1 m/s and D=1000 m) were concluded through S/N ratio.
- ANOVA results confirmed load (71.88 %) as the most influencing parameter on wear rate, whereas sliding distance (8.23 %) and sliding velocity (3.45 %) showed nominal influence.
- At low loads and velocities, wear was limited due to interfacial bond strengthening provided by Ni coating on TiC.
- Worn surface analysis revealed surface damages like protrusions, minor to severe delamination, grooves on HT composite specimen.

Tribology studies can be further explored at higher temperature for non-heat-treated and heat-treated Ni-coated TiC reinforced composites under variation in process parameters. The wear behavior under abrasive and reciprocating conditions can also be explored.

REFERENCES

[1] ASM International Handbook Committee, *Properties and Selection, Nonferrous Alloys and Special-Purpose Materials*, vol. 2, pp. 1143-1144, 1990, doi: 10.31399/asm.hb.v02.9781627081627

[2] E. Vandersluis, C. Ravindran, *Relationships Between Solidification Parameters in A319 Aluminum Alloy,* Journal of Materials Engineering and Performance, vol. 27, pp. 1109-1121, 2018, doi: 10.1007/s11665-018-3184-2

[3] M.G. Akhil, S. Preenu, S. Hari, M. Ravi, *Effect of Heat Treatment on the Mechanical Properties of Squeeze-Cast Al-5Si-3Cu Alloy for Automotive Applications*, Transactions of the Indian Institute of Metals, vol. 72, pp. 1129-1132, 2019, doi: 10.1007/s12666-019-01562-x

[4] M. Malekan, S.G. Shabestari, *Effect of Grain Refinement on the Dendrite Coherency Point During Solidification of the A319 Aluminum Alloy,* Metallurgical and Materials Transactions A, vol. 40, pp. 3196-3203, 2009, doi: 10.1007/s11661-009-9978-y

[5] E. Jayakumar, J.C. Jacob, T.P.D. Rajan, M.A. Joseph, B.C. Pai, *Processing and Characterization of Functionally Graded Aluminum (A319)— SiCp Metallic Composites by Centrifugal Casting Technique,* Metallurgical and Materials Transactions A, vol. 47, pp. 4306–4315, 2016, doi: 10.1007/s11661-016-3558-8

[6] P. Garg, P. Gupta, D. Kumar, O. Parkash, *Structural and Mechanical Properties of Graphene Reinforced Aluminum Matrix Composites,* Journal of Materials and Environmental Science, vol. 7, no. 5, pp. 1461-1473, 2016.

[7] B.V. Ramnath, C. Elanchezhian, R.M. Annamalai, S. Aravind, T.S. Atreya, V. Vignesh, C. Subramanian, *Aluminium Metal Matrix Composites–A Review*, Review on Advanced Material Science, vol. 38, no. 5, pp. 55-60, 2014.

[8] A.R. Kennedy, A.E. Karantzalis, S.M. Wyatt, *The Microstructure and Mechanical Properties of TiC and TiB_2-Reinforced Cast Metal Matrix Composites.* Journal of Materials Science, vol. 34, pp. 933-40, 1999, doi: 10.1023/A:1004519306186

[9] N. Samer, J. Andrieux, B. Gardiola, N. Karnatak, O. Martin, H. Kurita, L. Chaffron, S. Gourdet, S. Lay, O. Dezellus, *Microstructure and Mechanical Properties of an Al – TiC Metal Matrix Composite Obtained by Reactive Synthesis,* Composites Part A: Applied Science and Manufacturing, vol. 72, pp. 50-57, 2015, doi: 10.1016/j.compositesa.2015.02.001

[10] K.S. Arunagiri, N. Radhika, *Studies on Adhesive Wear Characteristics of Heat Treated Aluminium LM25/AlB_2 Composites*, Tribology in Industry, vol. 38, no. 3, pp. 277-285, 2016.

[11] N. Radhika, R. Raghu, *Evaluation of dry Sliding wear characteristics of LM 13 Al/B_4C composites*, Tribology in Industry, vol. 37, no. 1, pp. 20-28, 2015.

[12] T.P.D. Rajan, R.M. Pillai, B.C. Pai, *Reinforcement Coating and Interfaces in Aluminum Metal Matrix Composite,* Journal of Material Science, vol. 33, pp. 3491-3503, 1998, doi: 10.1023/A:1004674822751

[13] J. Mehta, V.K. Mittal, P. Gupta, *Role of Thermal Spray Coatings on Wear, Erosion and Corrosion Behavior: A Review*, Journal of Applied Science and Engineering, vol. 20, no. 4, pp. 445-452, 2017, doi: 10.6180/jase.2017.20.4.05

[14] L. Fan, Q. Wang, P. Yang, H. Chen, H. Hong, W. Zhang, J. Ren, *Preparation of Nickel Coating on ZTA Particles by Electroless Plating*, Ceramics International, vol. 44, iss. 10, pp. 11013-11021, 2018, doi: 10.1016/j.ceramint.2018.03.055

[15] S. Zou, X. Zhou, Y. Rao, X. Hua, X. Cui, *Corrosion Resistance of Nickel-Coated SiCp/Al Composites in 0.05m NaCl Solution*, Journal of Alloys and

Compounds, vol. 780, pp. 937-947, 2019, doi: 10.1016/j.jallcom.2018.10.245

[16] S. Hossain, M.M. Rahman, D. Chawla, A. Kumar, P.P. Seth, P. Gupta, D. Kumar, R. Agrawal, A. Jamwal, *Fabrication, Microstructural and Mechanical Behavior of Al-Al_2O_3-SiC Hybrid Metal Matrix Composites*, MaterialsToday: Proceedings, vol. 21, pp. 1458-1461, 2020, doi: 10.1016/j.matpr.2019.10.089

[17] A.M. Davidson, D. Regener, *A Comparison of Aluminium-Based Metal-Matrix Composites Reinforced with Coated and Uncoated Particulate Silicon Carbide,* Composites Science and Technology, vol. 60, iss. 6, pp. 865-869, 2000, doi: 10.1016/S0266-3538(99)00151-7

[18] C. He, Q. Zhou, J. Liu, X. Geng, Q. Cai, *Effect of Size of Reinforcement on Thickness of Anodized Coatings on SiC/Al Matrix Composites*, Materials Letter, vol. 62, iss. 16, pp. 2441–2443, 2008, doi: 10.1016/j.matlet.2007.12.016

[19] A. Urena, J. Rams, M. Campo, M. Sanchez, *Effect of Reinforcement Coatings on the Dry Sliding Wear Behaviour of Aluminium/SiC Particles/Carbon Fibres Hybrid Composites*, Wear, vol. 266, iss. 11-12, pp. 1128–1136, 2009, doi: 10.1016/j.wear.2009.03.016

[20] M.A. Sohag, P. Gupta, N. Kondal, D. Kumar, N. Singh, A. Jamwal, *Effect of Ceramic Reinforcement on the Microstructural, Mechanical and Tribological Behavior of Al-Cu Alloy Metal Matrix Composite*, MaterialsToday: Proceedings, vol. 21, pp. 1407-1411, 2020, doi: 10.1016/j.matpr.2019.08.179

[21] K. Bandil, H. Vashisth, S. Kumar, L. Verma, A. Jamwal, D. Kumar, N. Singh, K.K. Sadasivuni, P. Gupta, *Microstructural, Mechanical and Corrosion Behaviour of Al–Si Alloy Reinforced with SiC Metal Matrix Composite*, Journal of Composite Materials, vol. 53, iss. 28-30, pp. 4215-4223, 2019, doi: 10.1177/0021998319856679

[22] K. Wang, H.Y. Jiang, Q.D. Wang, B. Ye, W.J. Ding, *Nanoparticle-Induced Nucleation of Eutectic Silicon in Hypoeutectic Al-Si Alloy*, Materials Characterization, vol. 117, pp. 41–46, 2016, doi: 10.1016/j.matchar.2016.04.016

[23] E. Sjölander, S. Seifeddine, *The Heat Treatment of Al-Si-Cu-Mg Casting Alloys,* Journal of Materials Processing Technology, vol. 210, iss. 10, pp. 1249–1259, 2010, doi: 10.1016/j.jmatprotec.2010.03.020

[24] N. Chawla, Y.-L Shen, *Mechanical Behavior of Particle Reinforced Metal Matrix Composites,* Advanced Engineering Materials, vol. 3, iss. 6, pp. 357–370, 2001, doi: 10.1002/1527-2648(200106)3:6<357::AID-ADEM357>3.0.CO;2-I

[25] A. Banerji, P.K. Rohatgi, W. Reif, *Role of Wettability in the Preparation of Metal-Matrix Composites - A Review,* Metals Technology, vol. 38, pp. 656-661, 1984.

[26] Z.H. Huang, Y.J. Zhou, T.T. Nguyen, *Study of Nickel Matrix Composite Coatings Deposited from Electroless Plating Bath Loaded with TiB_2, ZrB_2 And TiC Particles for Improved Wear and Corrosion Resistance,* Surface and Coatings Technology, vol. 364, pp. 323–29, 2019, doi: 10.1016/j.surfcoat.2019.01.060

[27] J.N. Balaraju, T.S.N. Sankara Narayanan, S.K. Seshadri, *Electroless Ni-P Composite Coatings,* Journal of Applied Electrochemistry, vol. 33, pp. 807-816, 2003, doi: 10.1023/A:1025572410205

[28] G.H. Zhang, J.X. Zhang, B.C. Li, C.A.I. Wei, *Characterization of Tensile Fracture in Heavily Alloyed Al-Si Piston Alloy*, Progress in Natural Science: Materials International, vol. 21, iss. 5, pp. 380–385, 2011, doi: 10.1016/S1002-0071(12)60073-2

[29] A. Kumar, M.Y. Arafath, P. Gupta, D. Kumar, C.M. Hussain, A. Jamwal, *Microstructural and Mechano-Tribological Behavior of Al Reinforced SiC-TiC Hybrid Metal Matrix Composite*, MaterialsToday: Proceedings, vol. 21, pp. 1417-1420, 2020, doi: 10.1016/j.matpr.2019.08.186

[30] M.K. Akbari, H.R. Baharvandi, K. Shirvanimoghaddam, *Tensile and Fracture Behavior of Nano/Micro TiB_2 Particle Reinforced Casting A356 Aluminum Alloy Composites*, Materials & Design, vol. 66, pp. 150–161, 2015, doi: 10.1016/j.matdes.2014.10.048

[31] N. Radhika, K. Sai Charan, *Experimental Analysis on Three Body Abrasive Wear Behaviour of Stir Cast Al LM 25/TiC Metal Matrix Composite*, Transactions of the Indian Institute of Metals, vol. 70, pp. 2233–2240, 2017, doi: 10.1007/s12666-017-1061-6

[32] E.M. Sharifi, F. Karimzadeh, M.H. Enayati, *Fabrication and Evaluation of Mechanical and Tribological Properties of Boron Carbide Reinforced Aluminum Matrix Nanocomposites*, Materials and Design, vol. 32, iss. 6, pp. 3263-3271, 2011, doi: 10.1016/j.matdes.2011.02.033

[33] A. Vencl, A. Rac, I. Bobić, Z. Mišković, *Tribological Properties of Al-Si Alloy A356 Reinforced with Al_2O_3 Particles*, Tribology in Industry, vol. 28, no. 1–2, pp. 27–31, 2006.

[34] R. Jojith, N. Radhika, *Friction and Sliding Wear Studies on Functionally Graded Al LM25/WC Composite*, in International Conference on Advances in Materials and Manufacturing Applications, 16-18th August, 2018, ICONAMMA 18, Bengaluru, IOP Conference Series: Materials

Science and Engineering, vol. 577, no. 1, doi: 10.1088/1757-899X/577/1/012159

[35] N. Radhika, R. Raghu, *Development of Functionally Graded Aluminum Composites Using Centrifugal Casting and Influence of Reinforcements on Mechanical and Wear Properties*, Transactions of Nonferrous Metals Society of China, vol. 26, iss. 4, pp. 905–916, 2016, doi: 10.1016/S1003-6326(16)64185-7

[36] F.M. Mwema, J.O. Obiko, T. Leso, T.O. Mbuya, B.R. Mose, E.T. Akinlabi, *Wear Characteristics of Recycled Cast Al-6Si-3Cu Alloys*, Tribology in Industry, vol. 41, no. 4, pp. 613-621, 2019, doi: 10.24874/ti.2019.41.04.13